White Paper XI

An Experimental Investigation of Some Reconnective-Healing Workshops via a Unique Subtle Energy Detector

by

William A. Tiller, Ph.D. and Walter E. Dibble, Jr., Ph.D.

Introduction

Background

Our last dozen years of experimental and theoretical research in the psychoenergetics science area[1-4] has revealed that there are two uniquely different levels of physical reality and not just our normal, electric charge, atom/molecule level. In nature, these two levels of uniquely different kinds of substance appear to function in either (a) the uncoupled state, where they do not interact with each other on a macroscopic level, or (b) the coupled state where they do partially interact with each other.

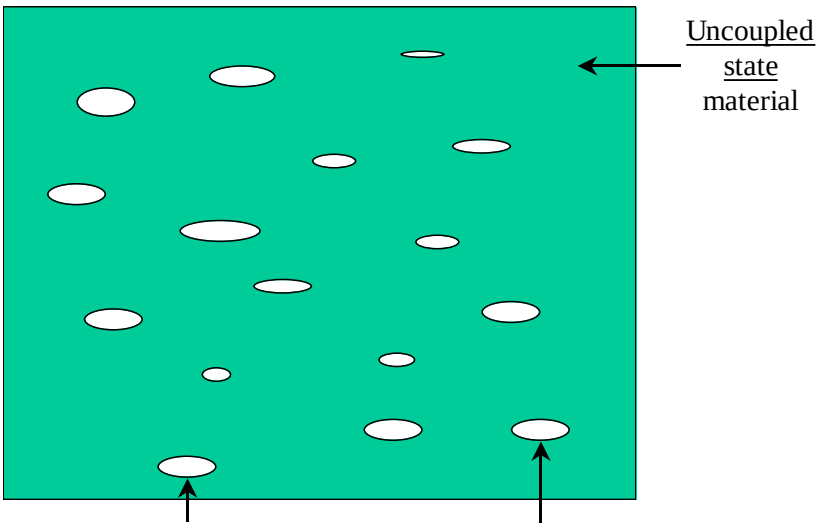

Figure 1. Nucleation and growth of the macroscopic coupled state of physical reality.

Figure 1 provides a schematic illustration of a macroscopic composite of these two uniquely different levels of physical reality. Here, the islands of the coupled state phase nucleate and grow within the uncoupled state host material (a room in a building, a piece of equipment, a piece of inorganic or organic material, etc.) via the application of a sufficiently strong field of human intention. If that intention field weakens, the size and number of the islands slowly shrink; when that intention field strengthens, the size of the islands slowly grow and the properties of the composite change according to the specific intention utilized in the experiment[1-4]. In our past experiments[1-4], a specific intention was mentally/emotionally embedded into a simple electronic circuit by a small group of people acting from a deep meditative state of consciousness. A small plastic

box containing this intention-host circuit was shipped to the experimental site where measuring equipment was continuously operating gathering uncoupled state property measurements of a high quality. This intention host device was placed a few feet from the experimental apparatus, plugged into an electric wall socket (power source) and switched on. For a 110 volt source the electrical power output of the box was less than one microwatt.

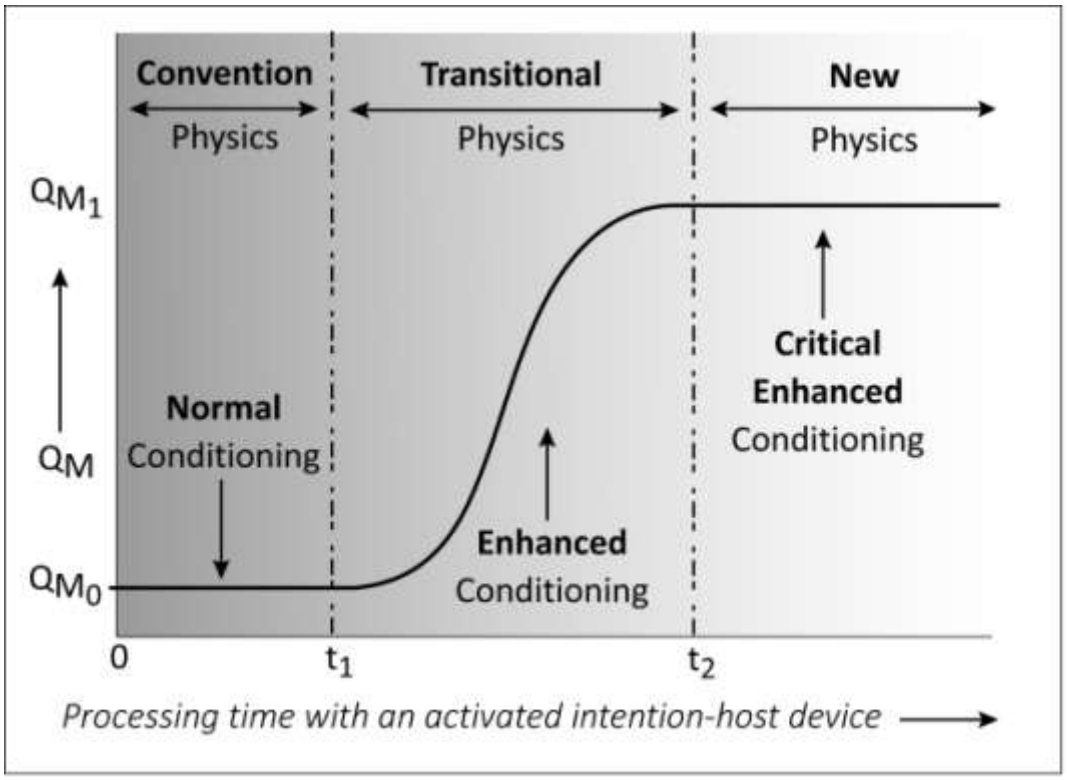

Figure 2. For any typical physical measurement, Q, the qualitative magnitude, Q_M, is plotted versus the degree of locale conditioning produced by continued intention-host device use.

Figure 2 illustrates the general time-dependence of the particular property measurement change as a function of space exposure-time to the corresponding imprint intention-host device. Here, we find that nothing much happens in the first 1-2 months (t_1=1-2 months), then the property measurement changes in a sigmoidal fashion, always in the direction intended, and asymptotically levels off, generally at the intended magnitude of change (t_2~3 months). In simple equation form, if $Q_M(t)$ is the magnitude of the property being measured, then we find that

$$Q_M(t) = Q_e + \alpha_{eff}(t)Q_m, \quad (1)$$

where Q_e is the uncoupled state magnitude of our electric charge atom/molecule world, Q_m is the uncoupled state magnitude of our physical vacuum, information wave world as influenced by the intention-host device, α_{eff} is the magnitude of the coupling coefficient between the two worlds and t is time. When $|\alpha_{eff}| \sim 0$, $Q_M \rightarrow Q_e$, our normal reality; when $0.05 \leq |\alpha_{eff}| \leq 1$, Q_M is appreciably changed either up or down according to the sign of the intention. Our present experimental data indicates that the specific intention alters only Q_m and not Q_e.

Four serious experiments have been reported on[1,2] and one has to date been replicated in ten different laboratories in the U.S. and Europe[3]. These are:

(1) To increase the pH of water in equilibrium with air by +1 pH units and with no intentional chemical additions,

(2) To decrease the pH of the same type of water in equilibrium with air by -1 pH units and with no intentional chemical additions,

(3) To significantly increase the in vitro thermodynamic activity of the liver enzyme alkaline phosphatase (ALP) via a 30 minute exposure to an intention-host device "conditioned" space and

(4) To significantly increase the in vivo ATP/ADP ratio in the cells of living fruit fly larvae via lifetime exposure (~28 days) to an intention-host device "conditioned" space so that they would become more physically fit and thus exhibit a significantly reduced larval development time, τ, to the adult fly stage.

All four of these experiments were robustly successful with #3 increasing ~25% to 30% at $p<0.001$ and with #4 (a) ΔATP/ADP increasing 15% to 20% at $p<0.001$ and (b) $\Delta\tau$ decreasing ~ -25% at $p<0.001$.

We utilized our pH-measurement system with a disk-shaped ceramic magnet placed symmetrically under the water vessel, first with one magnetic pole pointing upwards into the water vessel for several days and then with the opposite pole pointing upwards for the same time period, in order to detect any differences between the uncoupled state space conditioning and the coupled state space conditioning. For the former, there was no change in pH for either polarity as one might expect because, in our normal physical reality, although we have electric monopoles of both + and – charge, we have

only magnetic dipoles and even numbered magnetic multipoles whose energy and force effects are independent of spatial orientation. However, for a coupled state space conditioning, the picture is quite different as illustrated via Figure 3.

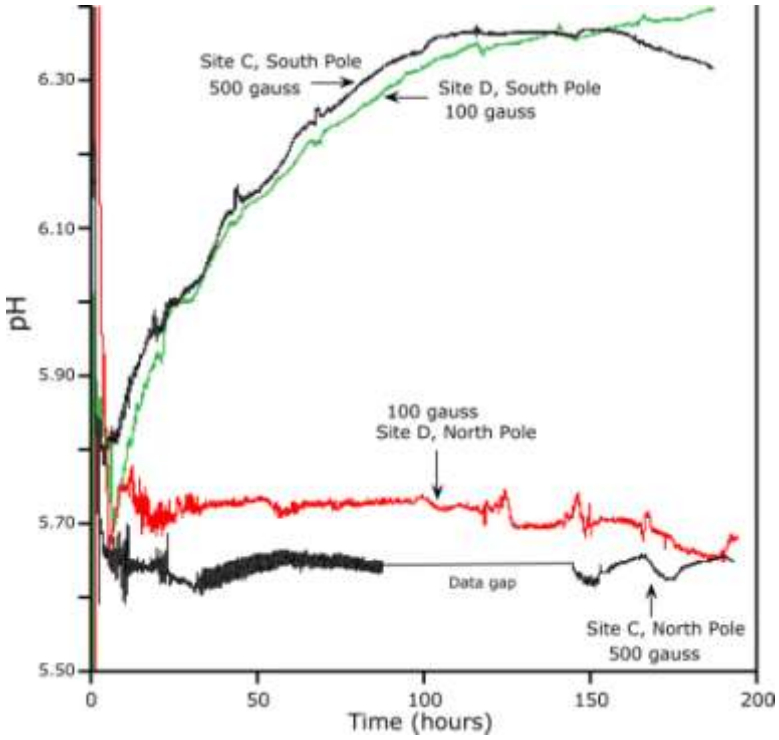

Figure 3. pH changes with time for pure water for both N-pole up and S-pole up axially aligned DC magnetic fields at 100 and 500 gauss.

This is the kind of result one would expect if the electromagnetic gauge symmetry state of the space had been lifted from the U(1) level for the uncoupled state space to the SU(2) level for a coupled state space where magnetic monopole charges appear to become accessible via pH-measurement instrumentation. Continued exploration of human subjects via the use of advanced kinesiological techniques and a world class kinesiologist[3], also demonstrated a DC-magnetic field polarity effect wherein the S-pole of a bar magnet held about 1 centimeter from a muscle-group on the body greatly strengthened the testing arm whereas the N-pole of the same magnet located in the same location greatly weakened the testing arm. We have deduced from this result that the human acupuncture meridian system is already functioning at the coupled state level of physical reality. Thus, an individual's specific unconscious or conscious intentions can modulate the flow of subtle energies (Qi) in their own meridians which, in turn, nourish the electromagnetic energy flows in their coarse (U(1) gauge) physical body.

Finally, to bring an end to this introductory background section, we found a theoretical procedure for calculating the excess

thermodynamic free energy change, δG_{H+}*, of the aqueous H^+-ion when an experimental space transitions from the uncoupled state to the coupled state of physical reality via use of an imprinted intention-host device.

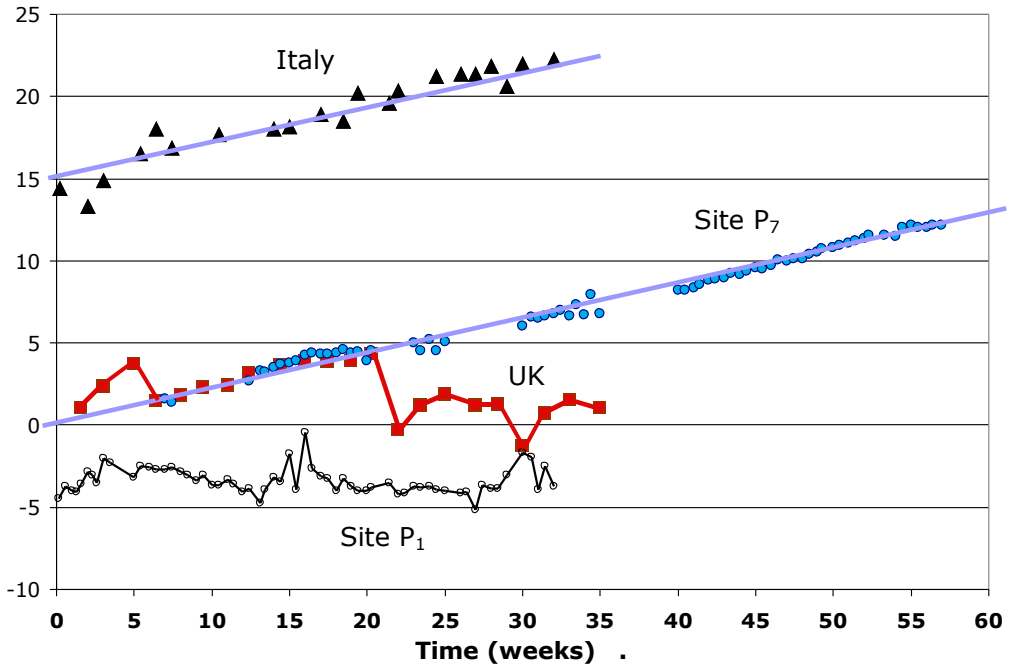

Figure 4. δG^*_{H+} vs. time at four diverse sites.

Figure 4 illustrates some gathered data for three of the ten sites involved in the replication experiment[3]. Here, two of the plots are from an active intention-host site (Payson, Arizona) and two are from control sites ~5000 miles to 6000 miles away where no intention-host device was ever present (U.K. and Italy). We found in this study[3] that serious spatial information entanglement occurs between active sites and control sites whether they are 100 meters, 2 to 20 miles, ~1500 miles or 6000 miles apart in spacetime without any ability to completely shield the control sites from the active sites. This type of information entanglement appears to be very different from quantum entanglement processes.

It is this particular type of subtle energy detector[6] that we will be using in our investigation of the Eric Pearl Reconnective Healing workshops in the pages to follow.

Subtle Energy Detection via pH-Measurement

Almost two decades ago, one of us[7] defined subtle energies as all those energies of nature beyond those creating the four fundamental forces of today's orthodox science (gravity, electromagnetism, the weak nuclear force and the strong nuclear force). So how can these subtle energies be detected and quantitatively measured? For this we need to recall Equation 1 and reference 6.

We start with the definition of pH as

$$pH=-\log_{10}(a_{H+}) \qquad (2a)$$

for the U(1) state where a_{H+} is the thermodynamic activity of the hydrogen ion, H^+, and $\log_{10}$ is the logarithm to the base 10. In experimental practice, Figure 5 provides a schematic set-up of the apparatus used in all of our test-site measurements[6], with the medium of investigation being some type of aqueous solution and a sensor probe involving both a pH-electrode and a water temperature sensor.

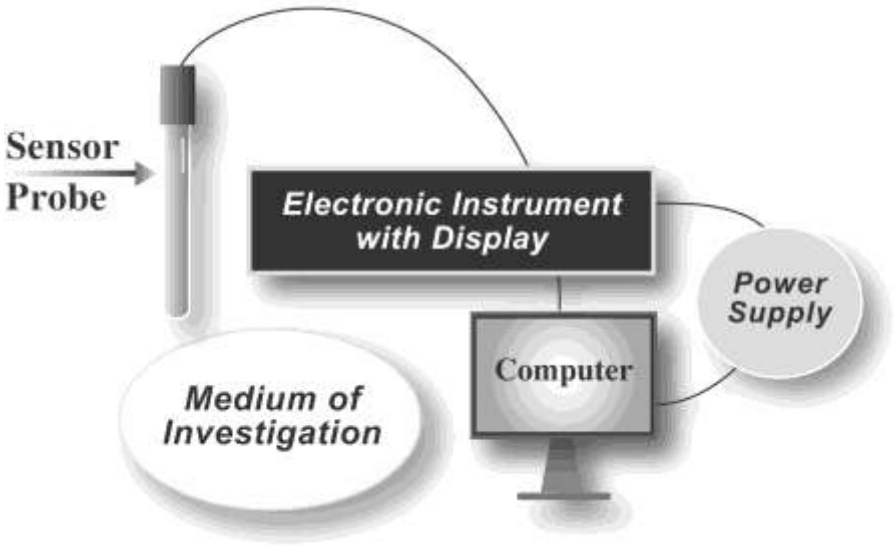

Figure 5. *Experimental set-up for testing pH changes.*

The physical aspect of pH measurement involves a device that connects (1) a unit H^+ activity standard chemical cell to (2) an aqueous solution vessel whose H^+ activity is to be measured via (3) an H^+-permeable membrane between (1) and (2). As the H^+-ion redistributes itself in this system to produce thermodynamic equilibrium throughout the system, an electric voltage, V_E, develops across the membrane/space charge interface.

The general Boltzmann equilibrium equation connecting V_E to $pH_{U(1)}$ can be readily calculated[6] to give, for an ideal system,

$$V_E=V_0\text{-}59.16pH\ (mV) \qquad (2b)$$

where V_0 is the standard cell voltage in the sensor of Figure 5. For the non-ideal case involving membrane interface polarization and other correction factors, Equation 2b becomes

$$V_E=S^*(pH_{U(1)}-7)T_{corr} \text{ where } T_{corr}=(T+273.15)/298.15. \qquad (2c)$$

Here, $V_0=7S^*$ and S^* is the electrode slope with respect to pH and voltage determined via calibration. Periodic determination of S^* by calibration is always required to attain accurate measurements.

Rearranging Equation 2c, we define the Nernst parameter, N, to honor that great physical chemist of the 1800's, where

$$N=\frac{S^*}{V_E}(pH-7)T_{corr}\,. \qquad (2d)$$

Of course, N should be equal to unity for the U(1) state (the uncoupled state of physical reality). However, as one "conditions" a space via an intention-host device from the U(1) gauge state to the SU(2) gauge state (the partially coupled state of physical reality as in Figure 1.), one finds that $N\neq1$ and that $|N-1|$ is a direct measure of $|\alpha_{eff}|$ in Equation 1.

For the partially coupled state of physical reality, the electromagnetic gauge symmetry state of the space is changing from the U(1) state towards the SU(2) state which is a higher thermodynamic free energy condition for the space. Thus, Equation 2c must be altered because Figure 6 now holds[6]. When one does this and follows the earlier theoretical procedure, one is able to take the pH-measurement data for the partially coupled state of a space and directly extract $\delta G_{H^+}{}^*(t)$-plots. This is exactly what we have done during our investigations of the four Reconnective-Healing workshops to follow.

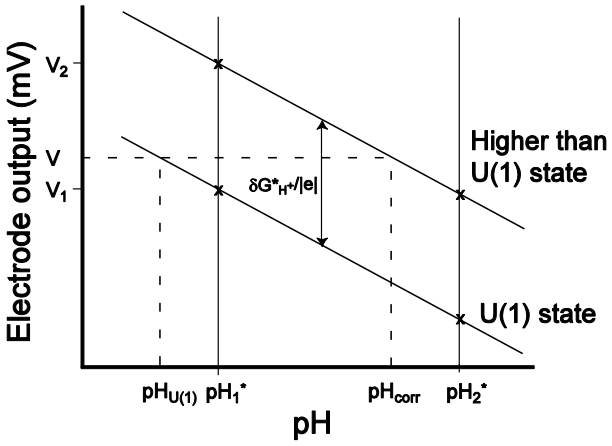

Figure 6. The electrode electrical output vs. pH plots for both the U(1) state ($\delta G^*=0$) and a higher than U(1) EM gauge symmetry state.

Experimental Protocols and Results

Test 1

Our first experimental test was at the Sedona workshop in February, 2006. Greg Fandel first tested the detector equipment in the Payson lab about 80 miles away and it performed well as had been our experience for several years at that site. He then drove the 1.5 hours to Sedona and set up the detector equipment in the large hotel room where the healing workshop was to take place about 5-6 hours later. Greg had difficulty in recalibrating the pH-measurement part of the system because the value of S in Equation 2c was falling outside the range of the normal pH calibration specifications. Eventually the system settled down to a degree so that pH and temperature measurements could commence. The next 9 hours of data-gathering is shown in Figure 7.

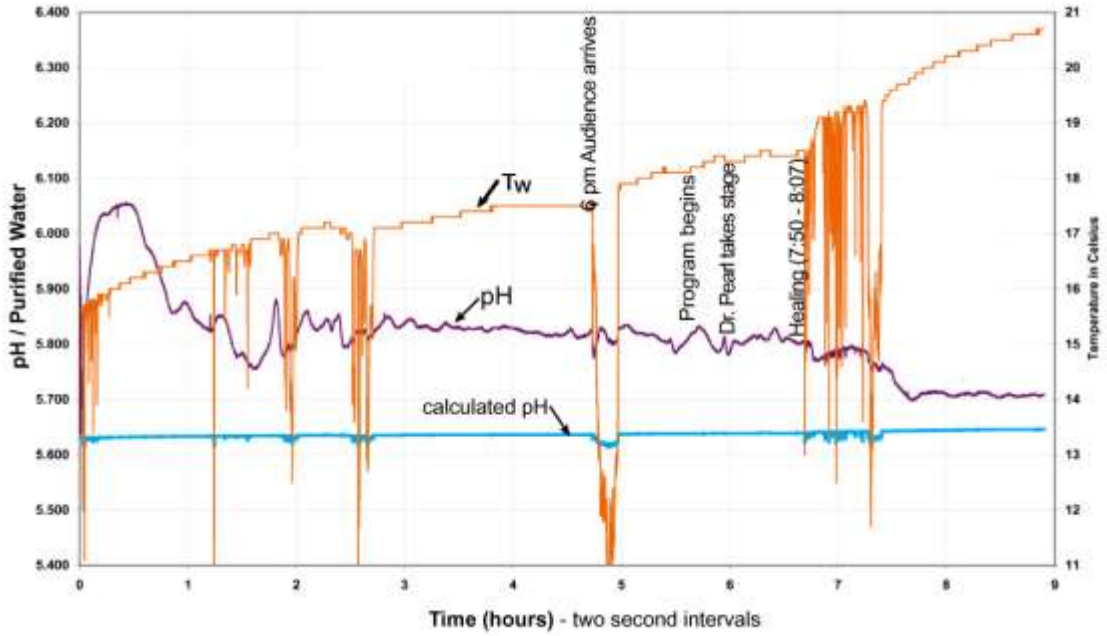

Figure 7. Very anomalous water temperature, T_W, behavior was observed at this Sedona, healing workshop.

Here, the uppermost curve, T_W, is the water temperature; the middle curve is the measured pH while the bottom curve is the theoretically calculated pH, $pH_{U(1)}$, which, following Equation 1 for both T_W and pH, are

$$T_M(t) = T_e(t)+\alpha_{eff}T_m, \quad (3a)$$

$$pH_M(t) = pH_{U(1)}(t)+\Delta pH_m(t), \quad (3b)$$

where

$$pH_{U(1)}(t)=5.54+3.12x10^{-3}T_e(t), \quad (3c)$$

and T_e is in ^oC. at an air CO_2 partial pressure of 380 ppm.

The T_W anomalies (downward shooting lines) in Figure 7 started to appear ~5 hours before the audience arrived in the large room and ended ~4 hours after they entered. These temperature measurement instabilities are revealed by the downward plunging lines in the T_W– plot. We have experienced this kind of phenomenon in our Payson lab

many times before and have found this type of anomaly to correlate strongly with the presence of high δG_{H+}*-values.

It is important for the reader to realize that this T_W –data indicates that this space had somehow been lifted to a very high EM gauge symmetry state well before any of the workshop participants entered that room (information entanglement in time??). When a pH-calibration cycle was carried out with the detector in this same room ~1 week after the workshop event, absolutely no anomalies at all appeared in either the T_W or pH plots and the room appeared to be completely back to its normal reality, the U(1) gauge symmetry state.

Analysis of this raw data to create a δG_{H+}*(t) plot occurred about 1.5 weeks later for this workshop room space. At time t=0, δG_{H+}* was found to be almost double what it would have been if α_{eff} in Equation 1 had been zero. At its peak (almost two days later) it had almost tripled the α_{eff}~0 value and, ~1.5 weeks later, it had decayed back to ~double again. If one asks the question "How much would one have had to "heat" this room from an α_{eff}=0 state to yield its maximum δG_{H+}*-state as found via our detector and describe the result as an effective temperature change, ΔT_{eff}, as given in Figure 8, one notes that it would have required a change in effective temperature over the workshop period by ~300 ^{0}C. However, the actual change in workshop room temperature was no more than ~5-10 ^{o}C. One implication of this result is that the δG_{H+}* occurring here is that due to an increased information creation process, which means a thermodynamic entropy decreasing rather that a thermodynamic energy increasing process, was taking place.

When I talked about a week or so later with one of the healers who had attended this workshop, she indicated that, during this workshop, her subjectively-assessed healing abilities felt as if they were ~3 to 5 times stronger than normal.

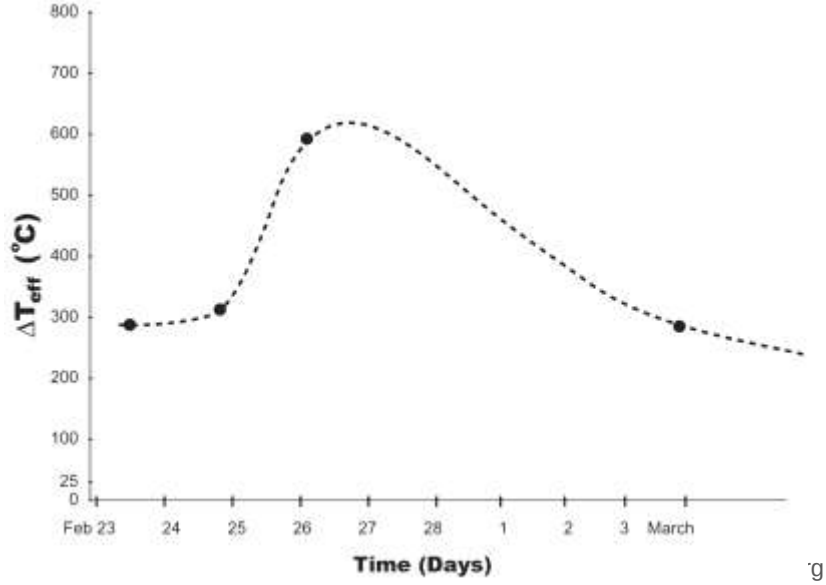

Figure 8. Possible data plot of the excess thermodynamic free energy for the healing workshop room as a function of time via converting δG^*_{H+} to an energy equivalent, effective change in temperature, ΔT_{eff}, for a normal room.

g

Test 2

Two complete sets of our standard T_W and pH measurement equipment plus a high resolution (0.001 $^oC.$) temperature probe for measuring air temperature, T_A, was driven from our Payson lab to the Sheraton Universal Hotel in Los Angeles (~500 miles) on July 25, 2007. The pH-electrodes were continuously kept in freshly purified water throughout the entire 8-day Payson/Los Angeles/Payson trip by Walter Dibble, Jr., except for when they were calibrated in L.A.

One of the main experimental goals was to quantitatively determine the existing degree of space conditioning above the purely U(1) gauge state prior to, during and after the main workshop events. One of the detector systems was set up on July 26 and continuously operated during the day in the Studio I room (for 2 days). Data, sampled at 10 second intervals was recorded via a laptop computer. This data revealed a pre-existing room space conditioning of ~-5± 1/2 meV (ΔT_{eff} ~60$^oC.$) was present at least two days prior to any workshop activity.

On the evening of July 27, this detector was moved to the Grand Ballroom (about 30 meters away from Studio I) in order to monitor Dr. Eric Pearl's evening lecture to the group of student healers convening for the following two-day workshop. Figure 9 provides simultaneous $T_W(t)$, $T_A(t)$and $\delta G_{H+}*(t)$ plots for a 5-hour period surrounding this event. Although, at 6:00 PM, the ballroom started out at $\delta G_{H+}*$~-6.5 meV, it had increased to ~-4.5 meV by the time the session actually began and, although T_A (and especially T_W) changed by no more than ~0.5 $^oC.$, ΔT_{eff} had changed by ~+20 $^oC.$ The relatively linear drop in

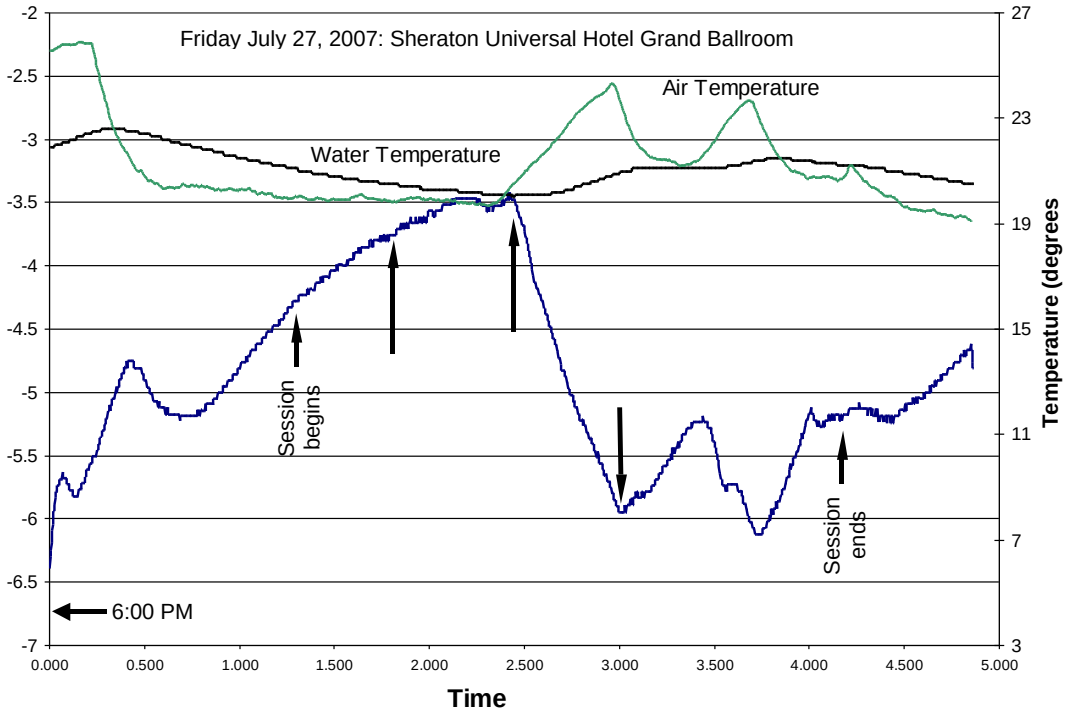

Figure 9. δG^*_{H+} for the space vs. time.

ΔT_{eff} by ~-30 ^oC. and increase in T_A by ~+4 ^oC., between 8:30 PM and 9:00 PM, when Dr. Pearl was performing subtle energy work onstage, appears to indicate that a Δ(TS) thermodynamic free energy term of the informational/entropic, S, type is strongly correlated with the process. One should also note, especially after 8:30 PM, how the δG_{H+}*-value is <u>more responsive</u> to T_A than to T_W. This may indicate a shift from pH-electrode "conditioning" to anti-phase space "conditioning".

On July 28 and 29, both detector systems were set up in the Studio I room to monitor the levels 1 and 2 workshops. Figure 10a, showing data for the 29th, indicates that each electrode has its own "personality" (depends on electrode history, make and manufacturer) with electrode I being more responsive than electrode II. Following the electrode data, one notices a strong correlation between the periods of an almost constant downward slope of δG_{H+}* with time when either Dr. Pearl or the teaching assistants were lecturing on stage. It appears as if an entrained coherence between the on-stage speaker and the audience is meaningfully controlling the pH-measurement equipment. This entrained coherence is broken via the speaker and audience moving about the room causing a reversal of any downward pH trend.

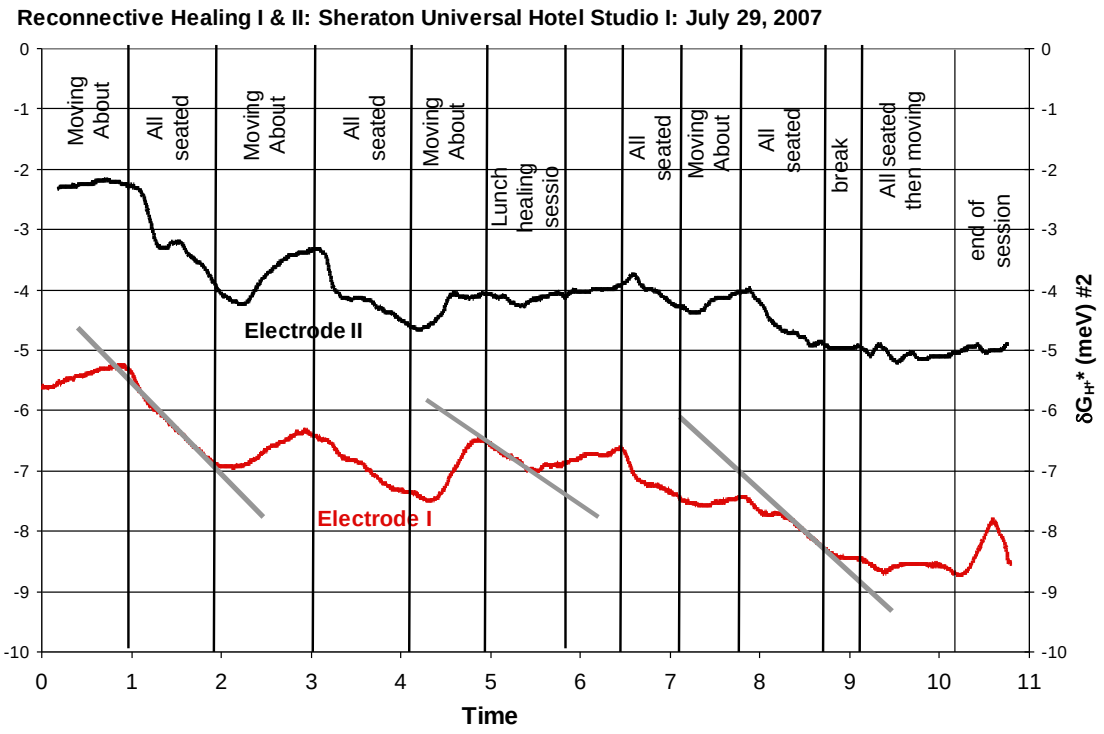

Figure 10a. δG^*_{H+} *for the space vs. time.*

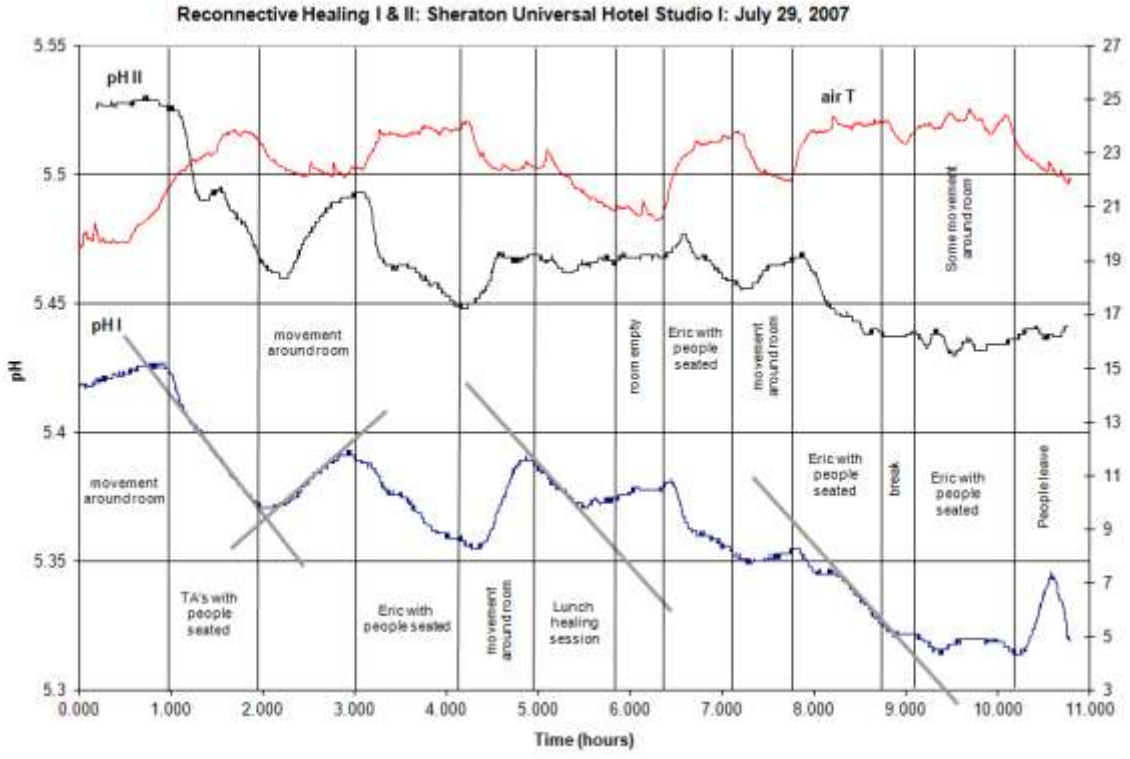

Figure 10b. pH (or δG^*_{H+}*) and air temperature vs. time.*

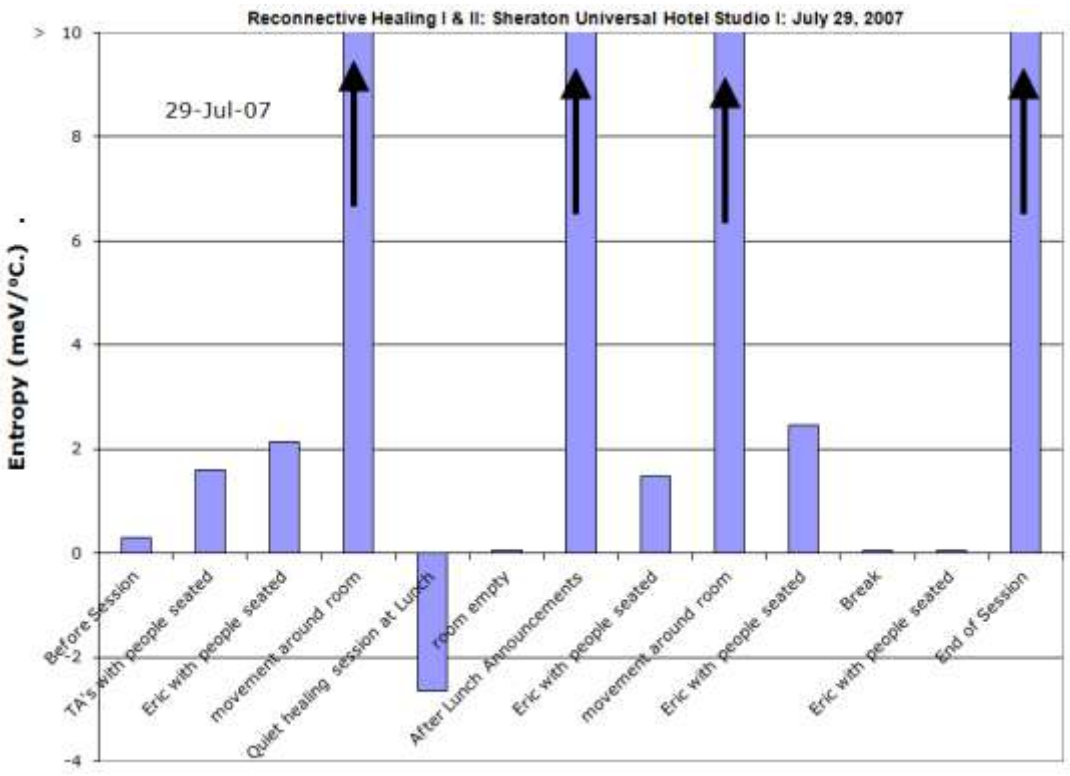

Figure 10c. Total entropy production vs. time.

From a thermodynamic perspective, the experimental results of this section require a modification of the Gibb's thermodynamic free energy expression to the form

$$G = PV + E - T\left(S_0 + \int_{t_1}^{t_2}(\delta S(t) + \delta I(t))dt\right) \qquad (4a)$$

where PV, E, T and S_0 are the standard pressure x volume, internal energy, temperature and initial entropy respectively, at time t_1 whereas our measurements extend over the period t_1 to t_2 where both some normal entropic processes occur and also information, I_1-created neg-entropy, $\Delta S = -\Delta I$, processes are assumed to occur. Differentiating G with respect to air temperature in Equation 4a leads to

$$\frac{dG}{dT} \approx -\left[S_0 + \int_{t_1}^{t_2}(\delta S(t) + \delta I(t))dt\right], \qquad (4b)$$

$$\approx \frac{d\left(\delta G^*_{H^+}/dt\right)}{(dT/dt)}. \qquad (4c)$$

From the derivative (slopes) of $\delta G^*_{H^+}$ (Figure 10a) and air T (Figure 10b), since the $\delta G^*_{H^+}(t)$ data comes from the pH(t)

experimental measurements, Equation (4c) can be solved. This allows one to evaluate the right-hand side of Equation (4b). Figure 10c provides us with a sum of both the positive and negative entropy contributions. Here, we observe that (a) the greatest positive entropy production occurs when there is significant human movement around the room both during and at the end of the session, (b) the **maximum** negative entropy period was during lunch when the room was used for private healing sessions and (c) three periods of negative entropy production large enough to reduce the total entropy production to almost zero.

Test 3

The Tucson, 2008 Level I and II workshop event occurred over the weekend of August 15-17 while the level III event occurred on the 18^{th} and 19^{th}, all at the Conference Center of the Sheraton Four Points Hotel. Three sets of our δG_{H+}*-detector and two high-resolution temperature probes were driven from Payson to Tucson with the pH-electrodes continuously in freshly purified water. One of the detector systems was eventually used with the pH-water bottle being open to the air while the other two were eventually used with the water bottle being closed to air. All the water had time to equilibrate with air before and during the trip to Tucson. The closed water bottles were to test for possible pH-variation that might result from variations in the CO_2 level present in the seminar rooms as people came and went during the day.

Figure 11, includes the Thursday pre-event measurements followed by a ~12 hour overnight disassembling and reassembling of the detector system at ~8 AM on Friday and at the big Friday evening event of Dr. Pearl's lecture. Once again we first see a small amount of supposedly pre-conditioning of the space on Thursday which is decaying towards zero. On Friday, the reassembled equipment starts

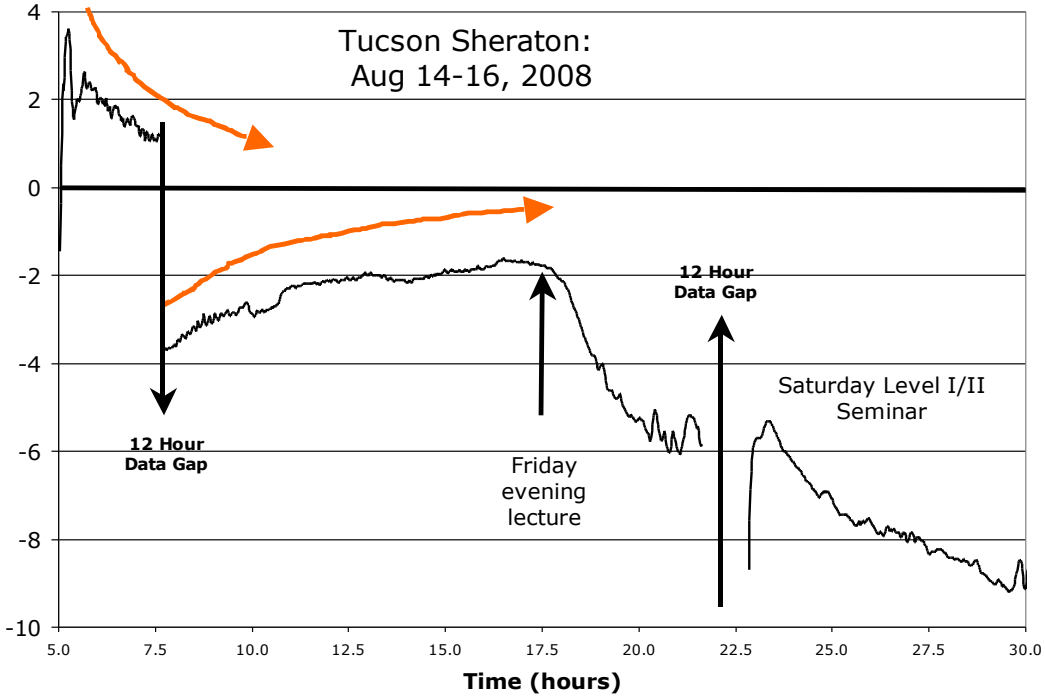

Figure 11. δG^*_{H+} *for the space vs. time. The curved arrows represent our best guess of where the data was headed before some significant change occurred.*

out with a pH of ~-4 meV which slowly diminishes in magnitude over time until the "Friday evening lecture" effect via Eric Pearl sets in. Once again the ~12 hour overnight detector system disassembling and Saturday morning reassembling occurs with the detector system seemingly picking up were it left off the previous evening and continuing its decrease in δG_{H+}* towards –9 meV.

The interesting Sunday, August 17 data shown in Figure 12 is very consistent with the Figures 10-data of July 29, 2007; however, two important factors need to be noticed here: (1) the very steep linear gradients in slope of δG_{H+}* with time during stage presentations in the afternoon are much larger in magnitude than for both the morning session and for the Figures 10 case and (2) a marked correlation exists between the two large blips in T_A and the two stage-presentation downward drops in δG_{H+}*. The similarities between the open-to-air pH water bottles and the air-tight pH water bottles strongly suggests that differences in spacetime air CO_2 levels are not being measured.

Test 4

The venue was the Universal Hilton in Los Angeles, September,

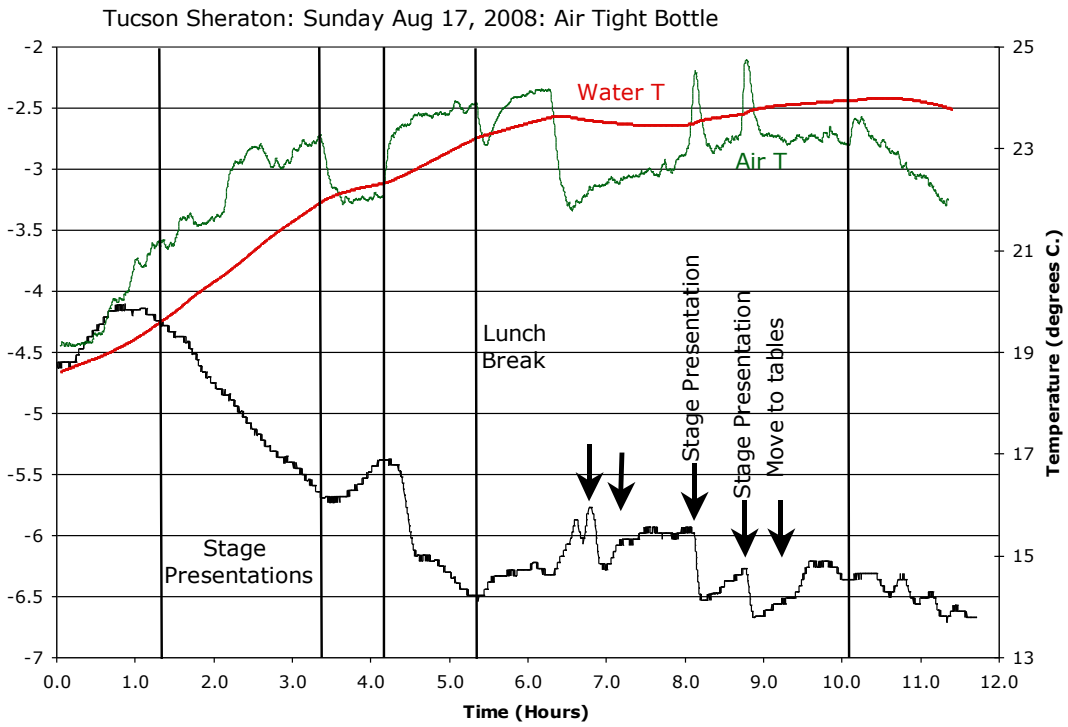

Figure 12. $\delta G^*_{H^+}$ for the space as well as water and air temperature vs. time.

2008. Once again, WED, Jr. drove a plethora of measurement equipment from our Payson Laboratory to Los Angeles. Four $\delta G^*_{H^+}$-detector systems and three high-resolution temperature probes were set up in the Plaza Suite room on Thursday September 11, 2008, one day before the Friday evening opening event. Figure 13 represents about 3 days worth of continuous data spaced out over a week. This data is similar to previous measurements of the "Friday Lecture Effect" with some notable new features. Most of the data gaps, once again, are due to the equipment being shut down and stowed overnight, then reactivated the next day. What is new here is the first 24-hour measurement in the Plaza Suite. This is the first time we were able to acquire a continuous 24-hour set of data (overnight) at one of these venues. After the electrode was calibrated at hour zero, there was roughly a 6-hour "settling in" period before the value leveled out. The value of ~−1.5 meV may actually represent the "real" background conditioning value for this room. The room was unoccupied for most of this 24-hour period. An interesting event occurred early in the morning on Friday (well before anyone entered the room) when there was a sudden break downward in $\delta G^*_{H^+}$-values with an almost linear slope. Could this be the onset of the "Friday Night Lecture Effect" starting at

this time? The equipment was then moved to the actual site of the Friday night lecture where the downward slope in δG^*_{H+}-values continued (even steeper) during the lecture event itself.

For the following two days (Saturday and Sunday) the trend in δG^*_{H+}-values was also strongly down during the measurement periods. The first strong uptrend to be observed in the measurements up to that time began near the end of the session on Sunday. The next day (Monday) the δG^*_{H+}-values started out much higher (following the trend of the previous days ending period?). Once again the curved arrows represent our best guess of where the data was headed before the equipment was shut down overnight. This data strongly suggests a return to zero space conditioning on Monday and Tuesday.

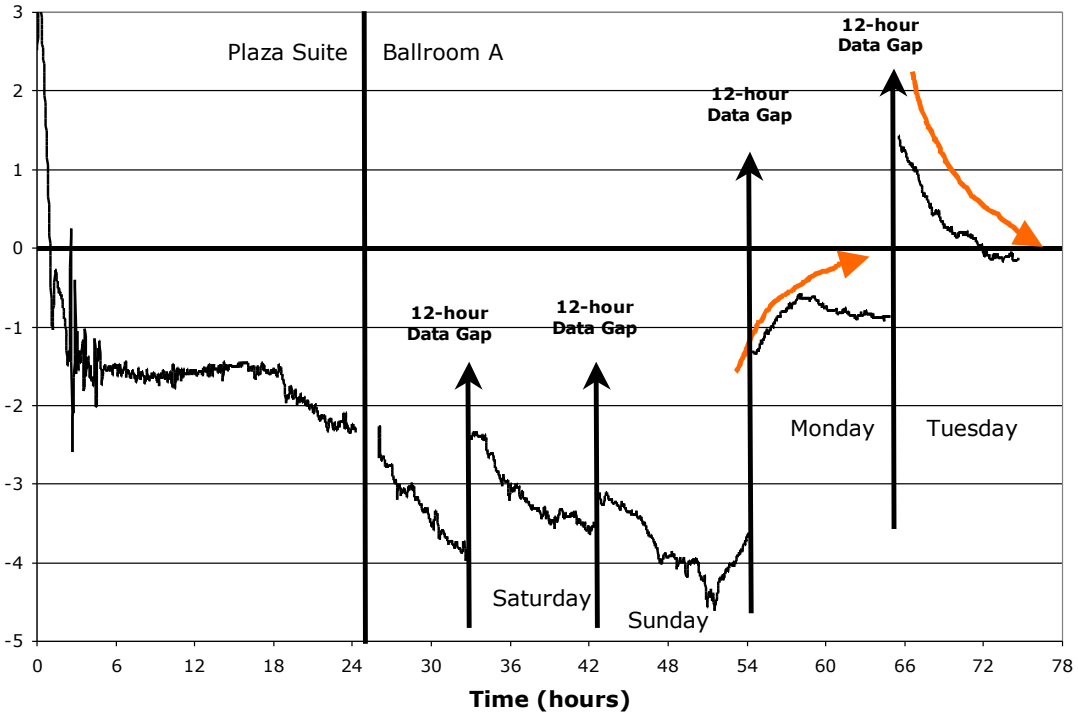

Figure 13. δG^*_{H+} for the space vs. time. The curved arrows represent our best guess of where the data was headed before the equipment was disassembled and reassembled.

Before closing this section, it is important to recognize that, as we have moved from Test 1 through Tests 2 and 3 to Test 4, we have steadily increased the multiplicity of individual measurement systems applied to the data-gathering process. Thus, the issue of information entanglement between these various individual sub-systems becomes important and one is in danger of "washing out" the magnitude of uniquely different effects via the out-of-phase coupling between different components of the overall measurement system. This is not a

problem for the various Q_e-parts in the Equation 1 mathematical formalism because they are basically scalar quantities (only one number is needed to define a property at a specific point in space). However, the individual factors that ultimately make up Q_m in Equation 1 are all vectors or tensors (one needs three or more numbers to define a property at a specific point in space) and these need to be added together in a special way (head to tail arrangement for vectors) even for one detector system. When there are four measurement systems operating simultaneously in the same space, the vector components of one detector information entangle with those of the other detectors because of the necessary vector addition and multiplication processes involved in the evaluation of Q_m and thus δG^*_{H+}. The mathematics is doable but tedious and not appropriate for this paper.

It is also appropriate to point out that, even within <u>one</u> detector system measuring the partially coupled state of physical reality, at least two kinds of "conditioning" need to be discriminated: (1) The pH-electrode change[6] and (2) a change in the room space itself relative to the uncoupled state reality. Thus, the <u>actual</u> measured value of δG^*_{H+} for a single detector, $\delta G^*_{H+}(M)$, is given by

$$\delta G^*_{H+}(M) = \delta G^*_{H+}(E) + \delta G^*_{H+}(s) \qquad (4)$$

where E refers to "electrode" and s refers to "space". It should be noted that, in Figure 4, δG^*_{H+} refers to $\delta G^*_{H+}(M)$ whereas in Figure 9 through 13, δG^*_{H+} refers to $\delta G^*_{H+}(s)$.

<u>Some Closing Observations and Comments</u>

1. During speaker on-stage presentations to the audience, one observes that the <u>magnitude</u> of δG^*_{H+} always seems to <u>increase</u> at ~ a constant slope with time. This signals positive information production and thus thermodynamic entropy annihilation,
2. During audience standing, moving around and talking, the magnitude of δG^*_{H+} always seems to <u>decrease</u>. This signals that net excess positive entropy production is occurring,
3. The periods of audience-focused attention upon the on-stage speaker signals that group entrainment leading to significant growth of group coherence is occurring. This leads to high information production rate events,
4. Substantial evidence was found for pre-event room "conditioning". Such events may be concrete examples of macroscopic temporal information entanglement,

5. Macroscopic spatial information entanglement due to simultaneous use of multiple measuring instruments appear to be generating reduced contrast in the magnitudes of various event signatures. This probably occurs via the addition of out-of-phase vector components (a type of data randomization) and
6. Clear highly correlated entrainment of $T_A(M)$ and $\delta G^*_{H+}(s)$ plots have been observed.

References

1. W. A. Tiller, W. E. Dibble, Jr., and M. J. Kohane, Conscious Acts of Creation: The Emergence of a New Physics (Pavior Publishing, Walnut Creek, CA, USA, 2001).
2. Tiller W. A., Dibble W. E. Jr., "New experimental data revealing an unexpected dimension to materials science and engineering", *Materials Research Innovations*, **5**, 21–34 (2001).
3. W. A. Tiller, W. E. Dibble, Jr. and J. G. Fandel, Some Science Adventures with Real Magic (Pavior Publishing, Walnut Creek, CA, USA, 2005).
4. W. A. Tiller, Psychoenergetic Science: A Second Copernican-Scale Revolution (Pavior Publishing, Walnut Creek, CA, USA, 2007).
5. W. A. Tiller, W. E. Dibble, Jr. and C. T. Krebs, "Instrumental response to advanced kinesiological treatments in a 'conditioned' space", *Subtle Energies and Energy Medicine*, **13** (2), 21-108 (2004).
6. W. A.Tiller and W. E. Dibble, Jr. "Toward general experimentation and discovery in "conditioned" laboratory and complementary and alternative medicine spaces: Part V. Data on 10 different sites using a robust new type of subtle energy detector". *J Altern Complement Med*, **13**, 133-149 (2007).
7. W. A. Tiller, "What are subtle energies?", *J. Sci. Expl.*, **7,** 293 (1993).